# **RSC Advances**



### **PAPER**

View Article Online
View Journal | View Issue



Cite this: RSC Adv., 2025, 15, 4693

# Chemical degradation as an enabling pathway to polymersome functionalization†

Chenyu Lin, (1) \*\* Kumar Siddharth (1) and Juan Pérez-Mercader (1) \*\*ab

Readiness and the ability to functionalize are the fundamental features of natural living systems. Understanding the chemical roots of functionalization is a basic guest for the generation of new materials in the laboratory and chemistry-based natural-life-mimicking artificial or synthetic living systems. Using polymerization-induced self-assembly (PISA) and starting from a homogeneous aqueous blend of a few strictly non-biochemical compounds, it is possible to create amphiphiles that can selfboot into submicron supramolecular objects (micelles). These micelles under the control of chemistry can undergo (1) morphological evolution into giant polymersomes and (2) exhibit growth-implosion cycles accompanied by (3) vesicle self-reproduction and population growth. We call the physicochemical processes underlying these life-like systems "Phoenix dynamics". Herein, we studied how the emergence of such functions in these systems can occur owing to the combination of the chemical degradation of the macro chain transfer agents involved in the PISA process due to the presence of oxygen and its impact on the physico-chemical evolution of these objects. Results indicated implications for the controllable degradation-triggered functionalization of self-booted synthetic supramolecular selfassembling systems and provided a physicochemical pathway to implement novel functionalities in supramolecular systems. Functionalization of polymersomes is of interest in many areas of science and technology, including biomedical and environmental applications and origins of life studies.

Received 3rd December 2024 Accepted 21st January 2025

DOI: 10.1039/d4ra08536a

rsc.li/rsc-advances

#### Introduction

Utilization of the degradation of polymers in terms of the chemical and physical modifications of their molecular structures has attracted a lot of attention in the fields of material science and chemistry in general.1 Investigating the degradation pathways in detail is important in the design of materials for applications in environmental and biomedical fields. 1-3 Interestingly, the degradation of chemical structures also plays an important role in the fields of origins of life studies and prebiotic chemistry.4 In this context, polymerization-induced self-assembly (PISA) is becoming a key method5,6 as it can resolve the problems associated with the 'arithmetic demon'7 and can be utilized to produce polymer vesicles (also called polymersomes), which are analogous to lipid bilayer vesicles.8 PISA is an extremely valuable technique that is compatible with several chemical reactions and has a diverse range of applications, including drug delivery, biomimetics and, importantly, the autonomous and chemically controlled generation of

Given the popularity, efficiency, scalability and diverse applications of PISA, it is important to understand the degradability aspects of materials involved in PISA reactions.11 For example, chemical degradation in PISA has been utilized to support controlled, order-order morphological transitions via a reductive degradation pathway,12 and it has been used in the context of reversible addition-fragmentation chain transfer (RAFT)-PISA to synthesize core-degradable polymer objects. 13 In an intriguing investigation, our group demonstrated the formation of polymersomes and their cyclic growth and collapse patterns (which we called "Phoenix dynamics") under the input of light energy.14 In a follow-up study, the mechanism behind this type of dynamic morphological transitions was further discussed. 15 It was pointed out that several factors that can affect the Phoenix dynamics are oxygen, irradiation, hydrated cores (nature of the monomers) and the presence of degradable chemicals and their byproducts. Hence, it is important to investigate and understand the chemical degradation characteristics of the macro-RAFT agent (m-RAFT) component of PISA, which plays a direct fundamental role in determining the resulting properties of the synthesized amphiphiles of the polymersomes undergoing Phoenix dynamics. It is also important to study the chemical degradation of the m-RAFT and its correlation and influence in the

polymersomes in one-pot reactors from a homogeneous blend of chemicals.  $^{8-10}$ 

<sup>&</sup>lt;sup>a</sup>Department of Earth and Planetary Sciences and Harvard Origins of Life Initiative, Harvard University, Cambridge, MA 02138-1204, USA. E-mail: chenyu\_lin@fas.harvard.edu; jperezmercader@fas.harvard.edu

<sup>&</sup>lt;sup>b</sup>Santa Fe Institute, Santa Fe, NM 87501, USA

functionalization process involved in the emergence of Phoenix dynamics.

In this paper we first discuss the experimental detail and characterization of the PISA system in a cuvette, followed by performing Phoenix dynamics studies *via* fluorescence microscopy. The significant implications of the Phoenix dynamics are established in terms of growth-implosion cycles and object count studies. The chemical degradation characteristics of mRAFT and the PISA system are then investigated with respect to the nature of m-RAFT, the oxygen levels, and the temperature effects, to provide a comprehensive and optimized analysis of the Phoenix dynamics.

#### Results and discussion

Fig. 1a shows the experimental procedure used for the photo-induced electron/energy transfer (PET)-RAFT-PISA experiments, which were carried out in a temperature-controlled cuvette, which was subsequently transferred to a microscope slide containing these photochemical reactions and then placed under a fluorescence microscope for studying the Phoenix dynamics. In brief, to begin with, the chemical reagents involved in PET-RAFT-PISA, *i.e.*, the m-RAFT, the water-soluble monomer HPMA (hydroxypropyl methacrylate), and the photocatalyst Ru(bpy) $_3$ Cl $_2$ , were mixed with 18 M $\Omega$  water to generate

a homogeneous chemical blend, which was then subjected to nitrogen bubbling for 15 min. The PET-RAFT polymerization was then carried out in a water-jacketed cuvette under blue-light continuous irradiation at 25  $^{\circ}$ C for 16 h.

The polymerization reaction was monitored *via* proton nuclear magnetic resonance spectroscopy analysis (¹H-NMR), as shown in Fig. S1.† The growing signals between 0.8–1.1 ppm (marked in red rectangles in Fig. S1a†) highlight the chain extension of the hydrophobic PHPMA block on the overall hydrophilic m-RAFT to form the amphiphiles, while Fig. S1b† portrays the progress of the degree of polymerization (DP) over time. In the reported experiments, the DP *vs.* time curve approached saturation beyond 8 h. Moreover, the final DP value of the PHPMA was around 20, which was relatively shorter than the 44 units of hydrophilic blocks (polyethylene glycol, PEG) of the amphiphiles. This chain extension of the hydrophobic PHPMA block on the m-RAFT agent with the hydrophilic PEG block endowed this diblock copolymer with amphiphilic properties.

Next, gel permeation chromatography (GPC) studies were conducted and the results are shown in Fig. S2,† showing the narrow molecular weight distribution and well-controlled chain extension of PHPMA achieved through the RAFT-mediated radical polymerization (the resulting polydispersity index, PDI, was 1.14 at the end of 16 h).

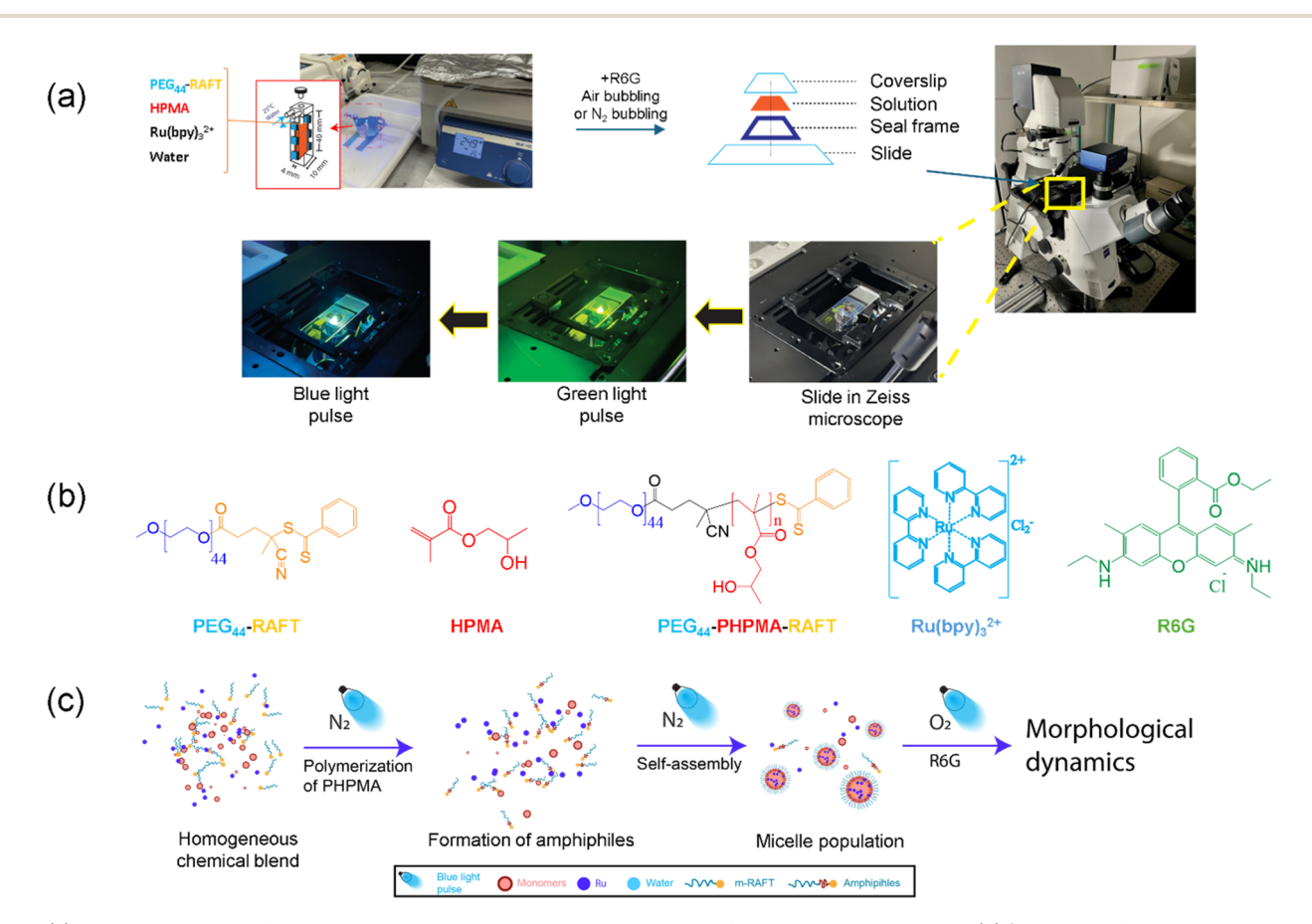


Fig. 1 (a) Experimental setup for the photochemical reactions in a cuvette and fluorescence microscope. (b) Structures of the chemicals used in the system. (c) Illustration of the PISA process and the subsequent morphological dynamics.

Paper

Using transmission electron microscopy (TEM) imaging (Fig. S3†), we found that the chain extension of PHPMA on the m-RAFT agent reached a concentration larger than the critical micelle concentration and they self-assembled into micelles (with sizes around 50 nm). The time evolution of the hydrodynamic diameter of the objects produced was also measured via dynamic light scattering (DLS) experiments, as illustrated in Fig. S4a.† The corresponding hydrodynamic diameter vs. time plot is displayed in Fig. S4b,† which shows the presence of nano-sized objects, which was in agreement with the TEM results. Similar to the DP, the average sizes of the selfassembled objects also reached saturation beyond 8 h. These characterization results fitted well with each other and suggest that our PET-RAFT PISA system conducted in the cuvette could autonomously boot-up as supramolecular systems to produce well-defined micelles with sizes in the nanoscale range.

The as-synthesized PISA suspension was then stained with rhodamine 6G dye (4 µM in the suspension), followed by a gentle air bubbling, and was then transferred to a framesealed microscopic slide. The ensuing photochemical reactions that took place in the PISA suspension were carried out using blue-light pulsed irradiation (on a Zeiss Axio Observer Z1 microscope using its 40× objective) for studying the Phoenix dynamics. Detailed descriptions of the materials, PET-RAFT-PISA synthesis, and other characterization techniques are provided in the ESI.† The structures of all the chemical reagents involved are shown in Fig. 1b, while the ultraviolet-visible (UVvis) spectra of the necessary components are presented in Fig. S5.† An important point to note is that the microscope's blue light ( $\lambda = 470 \text{ nm}$ ) was used to carry out the photochemical reactions since it is would be absorbed primarily by the photocatalyst, Ru(bpy)<sub>3</sub>Cl<sub>2</sub>, while a green light pulse was used for imaging as the dye, rhodamine 6G, absorbs strongly in that region. An overall illustration showing the PISA process and the subsequent experimental workflow for Phoenix dynamics is presented in Fig. 1c.

With the energy supplied from the microscopic blue light into the closed slide chamber, the PISA suspension within it was expected to undergo chemical degradation in the presence of oxygen and exhibit active morphological dynamics, which we have previously called "Phoenix dynamics". 14,15 The fundamental mechanism behind the chemical degradation and the subsequent dynamic morphological evolution requires reactive which oxygen species (ROS), are generated photosensitization<sup>16-18</sup> of the photocatalysts in the system. These ROS react with the labile chemical bonds of the molecules in the micelle cores, leading to structural degradation inside the core. This degradation induces both a subsequent osmotic imbalance as well as packing defects of the micelles, which induces periodic growth and collapse while the Phoenix dynamics take place. Two basic stages constitute the Phoenix dynamics. The first stage involves a morphological transition from the micelles and is accompanied by size growth. The above osmotic imbalance creates a water influx, which forces the internal packed amphiphiles to reconfigure and form inverted micelles in the cores. Meanwhile, the packing defects enhance the water permeability, which promotes greater water influx and

the growth and merger (coalescence) of the internal inverted micelles. Eventually the inverted micelles in the cores form a single water lumen encapsulated by a single bilayer membrane. Through this process, the nano-sized micelles grow and transit to a giant vesicle morphology. During the second stage, the giant vesicles formed in the first stage exhibit active growth-implosion cycles with the progression of chemical degradation. As the vesicle lumen keeps expanding due to water influx, the membrane becomes thinner and, owing to the defects, also weaker. The expansion in pressure due to the acceleration of the vesicle membrane growth competes with the surface tension, ultimately leading to cavitation. In fact, these dynamics of polymersomes in aqueous solution can be thought of as a spherical bubble forming in an incompressible fluid, i.e., water in our case. Their evolution, under the assumption of spherical symmetry, can be described by the Rayleigh-Plesset equation, 19 which tells us that the competition of forces just described leads to cavitation and that once a critical maximum size is reached, the membrane will implode. Remarkably, this growth-implosion pattern was repeated for several cycles.

To investigate the above in more detail, the evolution of the diameter of one vesicle with the irradiation time was observed, and is shown in Fig. 2a. A trace for a specific object moving in the solution is presented in Fig. S6.† We found that the diameter gradually grew with time until a certain radius was achieved, and then it was drastically reduced in a short period of time, suggesting implosion of the membrane. Over time, the diameter of this particular polymersome started another growth cycle, followed again by its implosion. This led to another crucial feature of the Phoenix dynamics illustrated in Fig. 2b, where the number of polymersomes in the analyzed field of view is plotted against time. The growth curve for the number of vesicles could be well fitted by a Hill function  $(n \approx 2)$ , whereby the population of vesicles grew slowly at the beginning, followed by a rapid increase, and then grew at a decreasing rate. The corresponding confidence band is also highlighted and it can be seen that it widens as time elapses. These features and implications of Phoenix dynamics are quite significant and are directly linked to the presence of chemical degradation, especially with respect to the active end of the m-RAFT, since this is internal to the membrane and constitutes the intrinsic part of the packed amphiphiles in the vesicles.

The various morphological variations observed during this two-stage Phoenix dynamics can be essentially understood as the consequence of the reconfiguration of the packed amphiphiles under osmosis-induced water influx when chemical degradation takes place. Since the m-RAFT is an integral part of the amphiphiles (containing the hydrophilic blocks as well as their tail group) and controls their self-assembly and packing attributes, we asked ourselves if the onset of Phoenix dynamics would be impacted if the m-RAFT agent used in the PISA process were to be less prone to chemical degradation. We already know from our previous work<sup>14,15</sup> that the 2-sulfur m-RAFT exhibits Phoenix dynamics. Thus, to further test our hypothesis, we instead utilized a 3-sulfur m-RAFT (poly(ethylene glycol)methyl ether (4-cyano-4-pentanoate dodecyl trithiocarbonate) to replace the 2-sulfur m-RAFT in our synthetic system.

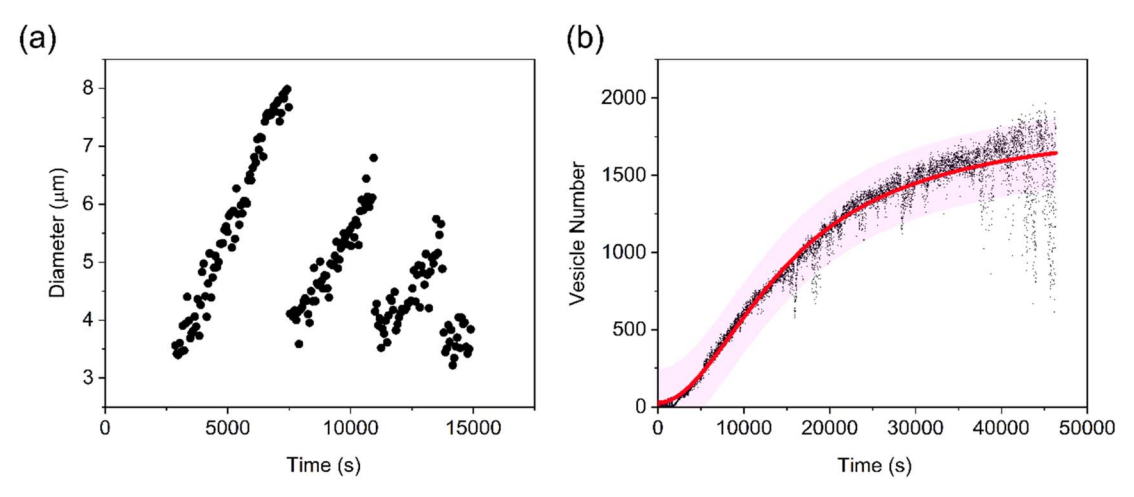


Fig. 2 (a) Diameter of the specific traced vesicle vs. time and (b) vesicle number vs. time curve.

It is known from the existing literature that the 3-sulfur m-RAFT is relatively more stable structurally than the 2-sulfur m-RAFT in an aqueous medium, <sup>20</sup> so we conducted the above experiments using 3-sulfur m-RAFT, while keeping all the other parameters and conditions the same. From the fluorescence microscopy images shown in Fig. S7,† it is clear that the system did not exhibit any observable Phoenix dynamics. This strongly corroborated our hypothesis that the nature of the m-RAFT, and hence the 2-sulfur m-RAFT agent, which is more easily degradable, is extremely significant for the existence of Phoenix dynamics.

We furthermore know that the chemical degradation of the 2-sulfur m-RAFT is strongly associated with the dissolved oxygen in the aqueous medium. Therefore, when degradation takes place, the m-RAFT agent losses its end-group, resulting in an irreversible decomposition of the thiyl radical species and the generation of small  $\mathrm{CS}_2$  and thiol species. The end-group of the m-RAFT molecule absorbs visible light (between 450 nm and 550 nm) through n to pi\* absorption, which aids the polymerization reaction, and, therefore, the reduction of absorbance in the UV-vis spectrum of an m-RAFT agent can be used to evaluate its degree of degradation.

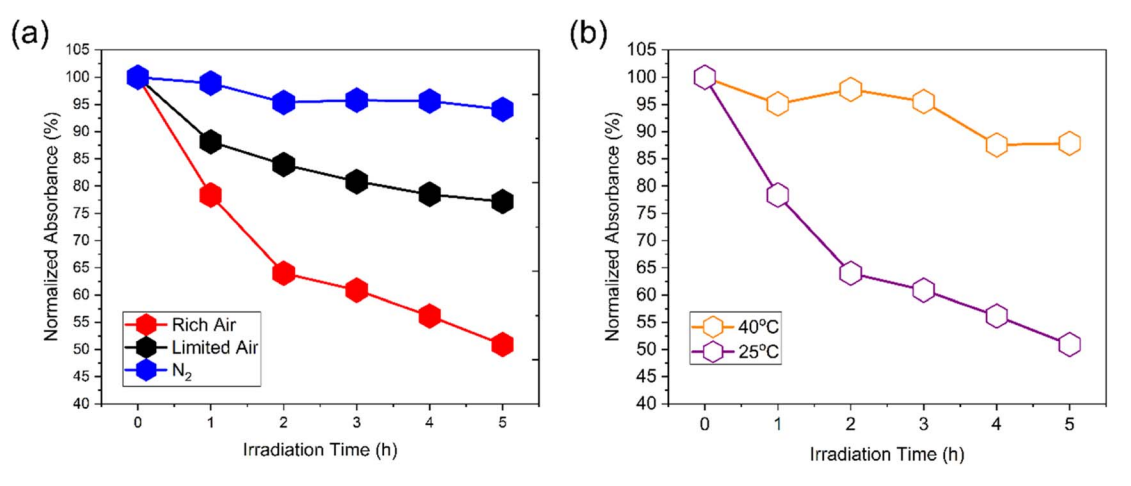
Next, we wanted to know whether the degree of chemical degradation of m-RAFT under various oxygen levels also influenced the Phoenix dynamics phenomenon. To test this, we first conducted tests involving chemical degradation of the 2-sulfur m-RAFT at 25 °C in three different environments: air bubbling (corresponding to a rich air/oxygen sample), nitrogen bubbling (corresponding to a minimum oxygen sample), and no bubbling (which we identified as a limited air/oxygen sample). The results for each of these scenarios are shown in Fig. 3a. For a normalized absorbance value, the absorption at each time point in the same curve was divided by the maximum absorption obtained before degradation (i.e., when the irradiation time was zero), and then expressed as a percentage. We can clearly see that the greatest degradation level was achieved in the rich air/oxygen sample, while the nitrogen-bubbled, i.e., minimum oxygen, sample showed little degradation, with a reduction in the UV-vis

absorption of less than 5%. Interestingly, the limited air/oxygen case not subject to any bubbling displayed an intermediate level of degradation. Put together, these results suggest that a sufficiently "abundant" oxygen supply is needed for chemical degradation in the system, and contributes to the degree of chemical degradation.

Armed with the above results related to the oxygendependent degradation of m-RAFT, we then further investigated its influence on the manifestation of Phoenix dynamics. For this, fluorescence microscopy images were obtained for three different PISA specimens, which were prepared following similar experimental protocols for all three oxygen conditions, as shown in Fig. S8.† For the minimum oxygen sample gelation, it was expected that, since the generation of ROS would be lowest, radical polymerization would dominate in the system due to the scarcity of dissolved oxygen. For the oxygen-rich sample, we observed the typical two-stage Phoenix dynamics, whereby the field of view of the microscope was full of giant vesicles executing Phoenix cycles. Meanwhile, for the limited oxygen case, we observed much fewer and small-sized objects in comparison to the rich-oxygen situation, suggesting a slow progress of the Phoenix dynamics. Considering the observed timescale for all scenarios, we could clearly conclude that the degree of dissolved oxygen and the chemical degradation characteristics of the m-RAFT were linked with regards to the progress of the Phoenix dynamics; whereby more oxygen led to a rapid chemical degradation of the 2-sulfur m-RAFT, and with it the faster progress of the Phoenix dynamics. The system thus displayed more well-defined giant vesicles. Overall, the labile chemical bonds of the m-RAFT, the amount of oxygen present, and the photocatalyst and dye,24 which contribute to the amplified synchronous chemical degradation of m-RAFT agents, were all key factors to consider with regards to the Phoenix dynamics performance of our PISA system.

Since it is known that the amount of dissolved oxygen is inversely proportional to temperature,<sup>25</sup> which in turn would affect the photoinduced degradation properties of a system, we next investigated how the Phoenix dynamics would be impacted

Paper



UV-vis studies for the degradation of the 2-sulfur m-RAFT agent (a) at various oxygen levels and (b) at 25 °C and 40 °C

by temperature. Fig. 3b shows a comparison of the UV-vis absorbance of the 2-sulfur m-RAFT agents with their degradation over with time (this is an irreversible process) at two temperatures, namely at 25 °C and 40 °C. Interestingly, the degradation of m-RAFT was much slower at 40 °C than at 25 °C, with an approximately only 10% reduction in absorbance after 5 h of irradiation. On the other hand, m-RAFT degraded rapidly at 25 °C, which could be due to the higher dissolved oxygen content. These two observations further underline the role of an oxygen-rich environment in efficient photodegradation. Subsequently, we explored the effect of these two temperatures on the progress of the Phoenix dynamics, as illustrated in Fig. 4. To understand and compare the Phoenix dynamics efficiency at the two temperatures (25 °C and 40 °C), we studied the average size and the count of the number of polymersomes produced  $\nu$ s. time within a fixed observable field of view. From the fluorescence microscopy images (Fig. 4a) at two different timepoints (12 648 s and 28 458 s) of our experiments, it can be seen that large well-defined vesicles rapidly filled the field of view at 25 °C, compared to at 40 °C. These observations were further confirmed by the analysis of the average polymersome size (Fig. 4c), which showed considerably higher average sizes at both timepoints for 25 °C. Considering the 2-stage mechanism of Phoenix dynamics, the self-assembled objects at 25 °C appeared to exhibit a more accentuated morphological transformation to vesicles and a faster size growth compared to the smaller sized and less prominent objects observed at 40 °C. This suggests a more rapid progress of the Phoenix dynamics at 25  $^{\circ}$ C than at 40 °C, since, as noted above, a larger amount of dissolved oxygen would lead to faster m-RAFT degradation. The faster Phoenix dynamics was also accompanied by a rapid growth of the object number. As can be seen in Fig. 4b, with the faster progress of the Phoenix dynamics at 25 °C, the object count also appeared to increase faster than at 40 °C before the timepoint of 12648 s. Despite this, when the large objects rapidly occupied a limited area in the field of view, the overall observable number increase slowed down over time and eventually reached a plateau. On the other hand, with the slower progress of the Phoenix dynamics at 40 °C, the objects started to

occupy the field of view at a slower and steadier rate than those at 25 °C after an initial small acceleration at a timepoint around 5000 s. Unlike the spatial limit that the large vesicles at 25 °C encountered, the smaller diameters of the emergent objects as a consequence of the slower Phoenix dynamics at 40 °C appeared to allow the spatially confined field of view to accommodate more small objects at the later stages of the experiment (after around 22 500 s). Given the average sizes and the growth observed prior to the spatial confinement of the field of view, the quicker degradation of the m-RAFT agent at lower temperature, like at 25 °C, could account for their contribution to accelerating the progress of the Phoenix dynamics.

## Summary

Overall, the features of the Phoenix dynamics were found to be strongly correlated with the chemical degradation of m-RAFT. As an inherent component of packed amphiphiles of the selfassembled objects, the degradation nature of the m-RAFT can affect and control the occurrence of the Phoenix dynamics. The oxidized tails of the amphiphiles within the hydrophobic phase of the vesicle (polymersome) membranes generated packing defects, which locally reduced the membrane tension, thus increasing the permeability of the polymersome membrane, and fostering an osmotic influx of water and then the subsequent morphological dynamics. This occurred due to the combined effects of the acceleration of the expanding membrane and the consequent change in membrane tension, together with changes in the average membrane-bound amphiphile's packing parameter. Therefore, the presence of chemical degradation is crucial for the existent physicochemical pathways to enable faster progress of the dynamic morphological transitions, which makes the choice of 2-sulfur m-RAFT significant. On this premise, the rich dissolved oxygen in the PISA system, coupled with the degradation with Ru photocatalyst and rhodamine 6G dye, contributed to enabling the functionalization of the polymersomes. Finally, as seen in the Phoenix phenomenon, the temperature affects the oxygen content in the solution, and hence the degradation of the m-

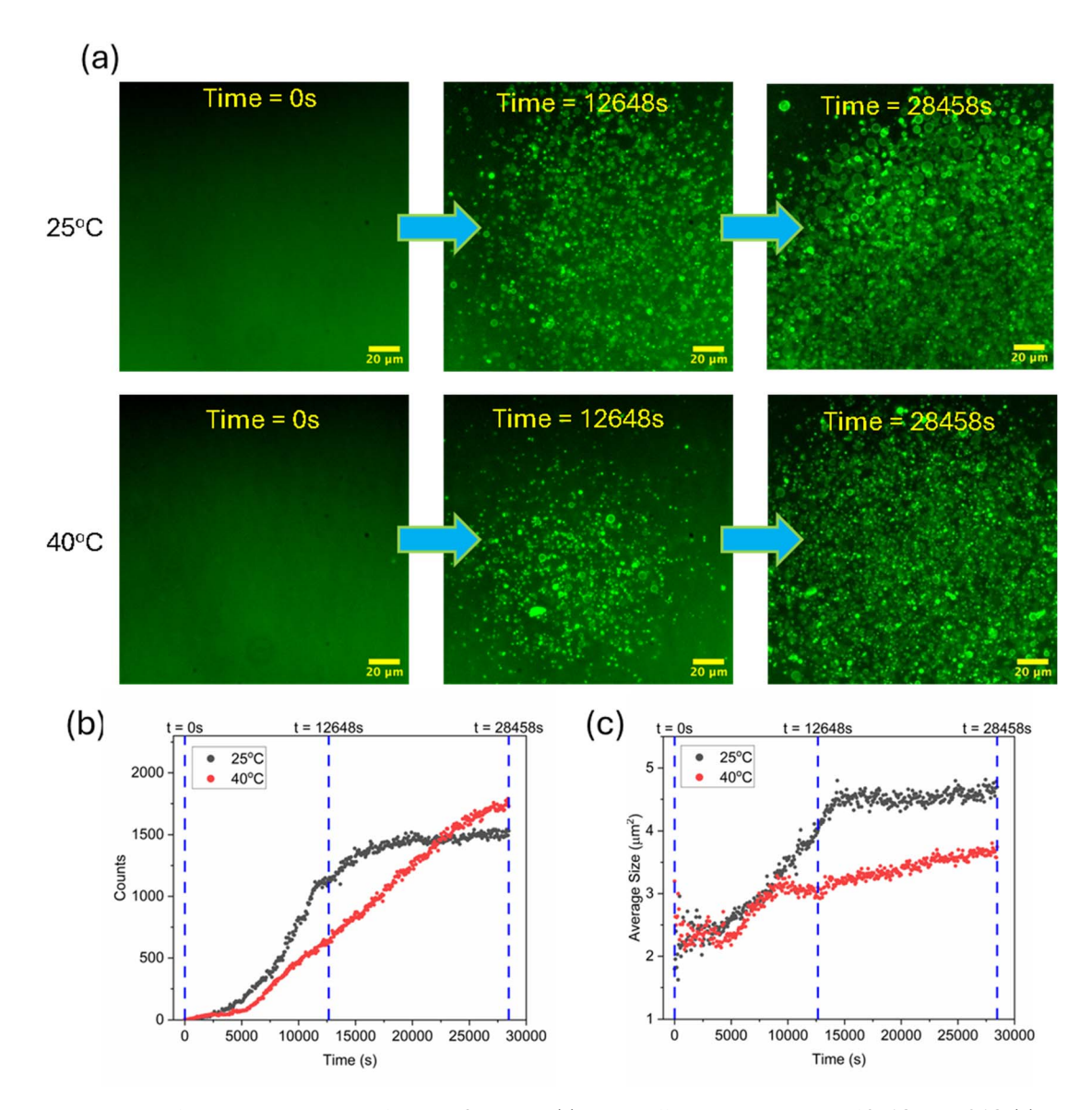


Fig. 4 Temporal evolution of the Phoenix dynamics for the PISA system (a) at two different temperatures of 25 °C and 40 °C, (b) their population growth trends, and (c) average size trends.

RAFT and the progress of the Phoenix dynamics. Thorough study of the m-RAFT degradation and Phoenix dynamic features enable us to elucidate a coherent pathway for optimized Phoenix systems and perhaps its extension to other systems, and to more generally illustrate the role that degradation can play in the development of functionality in self-booted synthetic supramolecular self-assembling systems.

#### Conclusions

Essentially, the intriguing two-stage Phoenix dynamics phenomenon is strongly related to the ongoing chemical degradation of m-RAFT since it is an intrinsic part of the packed amphiphiles. The degradation nature of m-RAFT determined whether we could observe Phoenix dynamics or not. Based on this proposition, the rich presence of dissolved oxygen and

amplified synchronous chemical degradation with a photocatalyst and dye pave the way for enhancement of the morphological dynamics, as well for functionalization of the polymersomes as a consequence of the chemical degradation. Importantly, the effect of temperature on the Phoenix dynamics was also investigated and could be explained *via* the degradation tests and microscopy analysis at two different temperatures.

# Data availability

The data used for writing this paper and reaching the conclusions reported in this study were collected by us in our laboratories using the instruments and general instrumentation facilities provided by our university, for which we were formally authorized as trained users. The data were obtained by the

respondand arr ESI† pupload Journal

Con
There

responsible use of the corresponding commercial instruments and are represented according to the protocols described in the ESI† provided along this manuscript. The raw data will be uploaded to the Harvard Dataverse website and reported to the Journal.

#### Conflicts of interest

There are no conflicts of interest to declare.

## Acknowledgements

We thank Repsol S. A. for their funding and the continued support for our work. We acknowledge the support from the Harvard Origins of Life Initiative in obtaining some of the equipment needed for this work. We thank the Harvard CNS (Center for Nanoscale Systems), a member of the National Nanotechnology Coordinated Infrastructure Network (NNCI), which is funded by the National Science Foundation of the United States under NSF award no. 1541959, for the infrastructure and support in TEM imaging. We also thank the Laukien-Purcell Instrumentation Center at Harvard for their support on the NMR. The funders had no role in study design, data collection and analysis, decision to publish, or preparation of the manuscript.

#### References

- 1 Q. Carboué, S. Fadlallah, M. Lopez and F. Allais, Progress in Degradation Behavior of Most Common Types of Functionalized Polymers: A Review, *Macromol. Rapid Commun.*, 2022, 43, 2200254, DOI: 10.1002/marc.202200254.
- 2 V. Delplace and J. Nicolas, Degradable Vinyl Polymers for Biomedical Applications, *Nat. Chem.*, 2015, 7(10), 771–784, DOI: 10.1038/nchem.2343.
- 3 R. R. Remya, A. Julius, T. Y. Suman, V. Mohanavel, A. Karthick, C. Pazhanimuthu, A. V. Samrot and M. Muhibbullah, Role of Nanoparticles in Biodegradation and Their Importance in Environmental and Biomedical Applications, *J. Nanomater.*, 2022, 2022(1), 6090846, DOI: 10.1155/2022/6090846.
- 4 A. P. Muñuzuri and J. Pérez-Mercader, Unified Representation of Life's Basic Properties by a 3-Species Stochastic Cubic Autocatalytic Reaction-Diffusion System of Equations, *Phys. Life Rev.*, 2022, **41**, 64–83, DOI: **10.1016/j.plrev.2022.03.003**.
- 5 S. D. P. Fielden, Kinetically Controlled and Nonequilibrium Assembly of Block Copolymers in Solution, *J. Am. Chem. Soc.*, 2024, **146**(28), 18781–18796, DOI: **10.1021/jacs.4c03314**.
- 6 A. Belluati, S. Jimaja, R. J. Chadwick, C. Glynn, M. Chami, D. Happel, C. Guo, H. Kolmar and N. Bruns, Artificial Cell Synthesis Using Biocatalytic Polymerization-Induced Self-Assembly, *Nat. Chem.*, 2024, 16, 564–574, DOI: 10.1038/ s41557-023-01391-y.
- 7 J. Pérez-Mercader, *De Novo* Laboratory Synthesis of Life Mimics without Biochemistry, *Artificial Life Conference*

- Proceedings, 2020, vol. 32, pp. 483-490, DOI: 10.1162/isal a 00282.
- 8 S. Pearce and J. Perez-Mercader, PISA: Construction of Self-Organized and Self-Assembled Functional Vesicular Structures, *Polym. Chem.*, 2021, **12**(1), 29–49, DOI: **10.1039/D0PY00564A**.
- 9 G. Cheng and J. Pérez-Mercader, Polymerization-Induced Self-Assembly for Artificial Biology: Opportunities and Challenges, *Macromol. Rapid Commun.*, 2019, **40**(2), 1800513, DOI: **10.1002/marc.201800513**.
- 10 N. J. W. Penfold, J. Yeow, C. Boyer and S. P. Armes, Emerging Trends in Polymerization-Induced Self-Assembly, ACS Macro Lett., 2019, 8(8), 1029–1054, DOI: 10.1021/ acsmacrolett.9b00464.
- 11 S. Zhang, R. Li and Z. An, Degradable Block Copolymer Nanoparticles Synthesized by Polymerization-Induced Self-Assembly, *Angew. Chem., Int. Ed.*, 2024, **63**(12), e202315849, DOI: **10.1002/anie.202315849**.
- 12 L. P. D. Ratcliffe, C. Couchon, S. P. Armes and J. M. J. Paulusse, Inducing an Order–Order Morphological Transition *via* Chemical Degradation of Amphiphilic Diblock Copolymer Nano-Objects, *Biomacromolecules*, 2016, 17(6), 2277–2283, DOI: 10.1021/acs.biomac.6b00540.
- 13 P. Galanopoulo, N. Gil, D. Gigmes, C. Lefay, Y. Guillaneuf, M. Lages, J. Nicolas, F. D'Agosto and M. Lansalot, RAFT-Mediated Emulsion Polymerization-Induced Self-Assembly for the Synthesis of Core-Degradable Waterborne Particles, *Angew. Chem., Int. Ed.*, 2023, 62(16), e202302093, DOI: 10.1002/anie.202302093.
- 14 A. N. Albertsen, J. K. Szymański and J. Pérez-Mercader, Emergent Properties of Giant Vesicles Formed by a Polymerization-Induced Self-Assembly (PISA) Reaction, *Sci. Rep.*, 2017, 7(1), 41534, DOI: 10.1038/srep41534.
- 15 C. Lin, S. K. Katla and J. Pérez-Mercader, Photochemically Induced Cyclic Morphological Dynamics *via* Degradation of Autonomously Produced, Self-Assembled Polymer Vesicles, *Commun. Chem.*, 2021, 4(1), 25, DOI: 10.1038/s42004-021-00464-8.
- 16 M. C. DeRosa and R. J. Crutchley, Photosensitized Singlet Oxygen and Its Applications, *Coord. Chem. Rev.*, 2002, 233– 234, 351–371, DOI: 10.1016/S0010-8545(02)00034-6.
- 17 A. B. Tossi and J. M. Kelly, A Study of Some Polypyridylruthenium(II) Complexes as DNA Binders and Photocleavage Reagents, *Photochem. Photobiol.*, 1989, 49, 545–556, DOI: 10.1111/j.1751-1097.1989.tb08423.x.
- 18 C. Nasr, D. Liu, S. Hotchandani and P. V. Kamat, Dye-Capped Semiconductor Nanoclusters. Excited State and Photosensitization Aspects of Rhodamine 6G H-Aggregates Bound to SiO<sub>2</sub> and SnO<sub>2</sub> Colloids, *J. Phys. Chem.*, 1996, 100(26), 11054–11061, DOI: 10.1021/jp9537724.
- 19 C. E. Brennen, *Cavitation and Bubble Dynamics*, Cambridge University Press, 2014.
- 20 A. W. Fortenberry, P. E. Jankoski, E. K. Stacy, C. L. McCormick, A. E. Smith and T. D. Clemons, A Perspective on the History and Current Opportunities of Aqueous RAFT Polymerization, *Macromol. Rapid Commun.*, 2022, 43(24), e2200414, DOI: 10.1002/marc.202200414.

- 21 I. O. L. Bacellar, M. C. Oliveira, L. S. Dantas, E. B. Costa, H. C. Junqueira, W. K. Martins, A. M. Durantini, G. Cosa, P. Di Mascio, M. Wainwright, R. Miotto, R. M. Cordeiro, S. Miyamoto and M. S. Baptista, Photosensitized Membrane Permeabilization Requires Contact-Dependent Reactions between Photosensitizer and Lipids, *J. Am. Chem. Soc.*, 2018, 140(30), 9606–9615, DOI: 10.1021/jacs.8b05014.
- 22 E. Yousif and R. Haddad, Photodegradation and Photostabilization of Polymers, Especially Polystyrene: Review, *SpringerPlus*, 2013, 2(1), 398, DOI: 10.1186/2193-1801-2-398.
- 23 G. McKenzie, T., M. Costa, L. P. da, Q. Fu, E. Dunstan and G. Qiao, G. Investigation into the Photolytic Stability of

- RAFT Agents and the Implications for Photopolymerization Reactions, *Polym. Chem.*, 2016, 7(25), 4246–4253, DOI: 10.1039/C6PY00808A.
- 24 C. Eggeling, A. Volkmer and C. A. M. Seidel, Molecular Photobleaching Kinetics of Rhodamine 6G by One- and Two-Photon Induced Confocal Fluorescence Microscopy, *ChemPhysChem*, 2005, **6**(5), 791–804, DOI: **10.1002/cphc.200400509**.
- 25 F. P. La Mantia, M. Baiamonte, S. Santangelo, R. Scaffaro and M. C. Mistretta, Influence of Different Environments and Temperatures on the Photo-Oxidation Behaviour of the Polypropylene, *Polymers*, 2023, 15(1), 74, DOI: 10.3390/polym15010074.